Appl Phys A (2011) 105:847–854
DOI 10.1007/s00339-011-6646-z

Applied Physics A
Materials Science & Processing

Multiple activation of ion track etched polycarbonate for the electroless synthesis of metal nanotubes

F. Muench · M. Oezaslan · T. Seidl · S. Lauterbach · P. Strasser · H.-J. Kleebe · W. Ensinger

Received: 15 June 2011 / Accepted: 6 October 2011 / Published online: 4 November 2011

Abstract In our study, we examined the formation of thin films of silver nanoparticles on polycarbonate and the influence of the silver loading on the electroless synthesis of metal nanotubes. Control of the silver film thickness occurred by consecutive dipping of the polymer template in tin(II) and silver(I) solutions. The deposition progress was studied using UV-Vis spectroscopy. The reaction mechanism relies on the adsorption of reactive ions on the polymer template as well as on the silver nanoparticles. The initial catalytic activity of silver-covered ion track etched polycarbonate is an important governing factor for the electroless synthesis of metal nanotubes with desired thickness and shape. Therefore, the presented method allows specific template preparation according to given synthetic demands. High aspect ratio copper, gold, and platinum nanotubes were produced by the combination of sufficiently activated templates with optimized electroless plating procedures.

F. Muench (✉) · T. Seidl · S. Lauterbach · H.-J. Kleebe · W. Ensinger
Department of Materials and Geoscience, Technische Universität Darmstadt, Petersenstraße 23, 64287 Darmstadt, Germany
e-mail: muench@ca.tu-darmstadt.de
Fax: +49-6151-166378

M. Oezaslan · P. Strasser
Department of Chemistry, Technische Universität Berlin, Straße des 17. Juni 124, 10623 Berlin, Germany

T. Seidl
Material Research Group, GSI Helmholtz Centre for Heavy Ion Research GmbH, Planckstraße 1, 64291 Darmstadt, Germany

1 Introduction

In the early 1990s, Martin and coworkers developed several methods for the template-supported synthesis of metallic micro and nanotubes (NTs), focusing on electroless plating and ion track etched polycarbonate [1–3]. Ion track etched polymer templates contain stochastically distributed channels whose density, diameter, and shape can be substantially varied by the production conditions [4–6]. Wires and tubes are obtained by depositing metals in these channels [7–10]. These virtually one-dimensional nanostructures have been effectively implemented in relevant fields such as nanoelectrochemistry [3], field emission [7], selective chemical transport [8] and flow-through [9], or fuel cell [10] catalysis.

In controlled reactions, electroless plating leads to a uniform metal deposition on the whole template surface. Therefore, it is especially suited for the homogeneous coverage of complex shaped templates such as nanochannel-containing membranes with extended inner surfaces. NTs are formed by deposition of a metal film on the nanochannel walls. Due to this growth mode, electroless plating is a straightforward method for the synthesis of tubular metal structures. In contrast, electrochemical plating leads to a linear growth of metal starting from the cathode side. This method prefers clearly the formation of wires [7]. Electroplating relies on the reduction of metal cations present in the plating solution by cathode-supplied electrons. In electroless baths, the reaction is maintained by a chemical reducing agent. These plating solutions are thermodynamically instable with respect to decomposition to the metal and a corresponding oxidation product [11, 12].

To obtain surface-selective deposition, the reaction must be kinetically suppressed in the bulk solution and enforced on the template surface. The first condition is met by introducing metastable redox pairs (an appropriate combination

of one or more metal sources, reducing agents and additives) which are insensitive toward homogeneous nucleation [11, 12]. Depending on the metal to be plated, various baths have been developed, comprising Co [14], Ni [14], Cu [13–15], Ag [16], Au [8, 9], Pd [17], or Pt [10]. The critical challenge is the stability of these baths [12, 13]. The second requirement is achieved by using templates which catalyze the decomposition reaction. After initiation of the electroless plating, the formed metal film sustains the deposition reaction by autocatalysis [11, 12]. The bare polymer templates mostly do not promote the deposition reaction. Therefore, an appropriate pre-treatment of polymer templates is of major importance for electroless plating. Usually, they are activated by anchoring Ag- [3, 9, 10] or Pd-nanoparticles (NPs) [13] on their surface. However, sparse effort has been spent on examining the nature of the Ag structures formed on polycarbonate templates as well as their reactivity in consecutive electroless plating. New methods to enhance and tune the activity of these templates are required to improve or to enable the challenging synthesis of high aspect ratio metal-NTs.

In general, the successful preparation of metal-NTs by electroless plating depends on the combination of a sufficiently activated substrate with a plating bath ensuring slow and controlled metal deposition. Activation as the starting point of the metal film growth is a crucial step for both the homogeneity and density of the obtained NTs [11], while low deposition rates are essential to ensure sufficient mass transport of the reactants to the poorly accessible regions inside the template [8, 14]. Additionally, the metal deposit has to be uniform on the nanoscale. In this work, we provide synthetic guidelines for the electroless fabrication of Au-, Pt-, and Cu-NTs using tailored Ag-NP activation.

2 Experimental details

General, chemicals All glassware was cleaned with aqua regia prior to use. All reaction solutions were freshly prepared. Following chemicals were used without further purification: 4-(dimethylamino)pyridine (Fluka, puriss.); silver nitrate (Grüssing, p.a.); ammonia 33% in water (Merck, puriss.); copper sulfate pentahydrate (Fluka, purum p.a.); ethylenediamine (Fluka, puriss. p.a.); formaldehyde solution 37% in water, methanol stabilized (Grüssing, p.a.); hexachloroplatinic acid 8% in water (Fluka); hydrazine hydrate 80% in water (Merck, for synthesis); methanol (Sigma-Aldrich, laboratory reagent); potassium sodium tartrate tetrahydrate (Fluka, puriss. p.a.); sodium chloride (Merck, suprapur); sodium hydroxide solution 32% in water (Fluka, puriss. p.a.); sodium sulfite (Merck, p.a.); tin(II) chloride (Merck, for synthesis); tin(II) methanesulfonate 50% in water (Sigma-Aldrich); trifluoroacetic acid (Riedel-de Häen, >99%). A commercial electroplating solution (El-Form Galvano Goldbad, Schütz Dental GmbH) was used as the Au source (15 g 99.9% Au per liter, present as $(NH_4)_3(Au(SO_3)_2)$). All procedures were conducted with purified water (Milli Q 18-MΩ water).

Template synthesis Polycarbonate foils (Makrofol®, Bayer MaterialScience AG, nominal thickness 30 µm) were irradiated with Au ions (energy: 11 MeV per nucleon; fluence: 1×10^8 ions per cm^2) at the GSI Helmholtz Centre for Heavy Ion Research (Darmstadt). Subsequently, they were irradiated with UV light in the presence of air (1 h per side, UV source provides 1.5 and 4 W m^2 in the range between 280 nm–320 nm and 320 nm–400 nm) and etched in stirred sodium hydroxide solution (6 M, 50°C, time depending on desired nanotube diameter). The as-prepared templates were thoroughly washed with purified water and dried in air before use.

Covering the template with Ag-nanoparticles Firstly, the etched polycarbonate membranes were stored in a Sn(II)-solution for at least 45 min (0.042 M $SnCl_2$, 0.071 M CF_3COOH in methanol:water = 1:1). To remove excessive Sn(II), the impregnated foils were washed twice with ethanol before immersing them in Ag(I)-solution for 3 min (0.059 M $AgNO_3$, 0.230 M NH_3). These procedures were performed at room temperature. For multiple activation, the templates were washed twice with ethanol prior to repeating the described procedure.

Electroless synthesis of metal nanotubes The last washing step before the transfer to the growth solution was conducted with ethanol, followed by water. All depositions took place at 8°C. After the desired reaction time, the metal-covered templates were taken out, washed with water and dried in air. Au and Pt deposition solutions were prepared according to reported procedures [9, 10]. They contained Au(I), sulfite, 4-(dimethylamino)pydidine and formaldehyde in the case of the Au solution and Pt(IV), chloride, ethylenediamine and hydrazine for the Pt solution. The Cu deposition solution contained 0.10 M Cu(II) (introduced as copper sulfate), 0.22 M tartrate (introduced as potassium sodium salt), 0.24 M ethylenediamine and 1.2 M formaldehyde. It was adjusted to a pH value of 11.5–12.0.

Analytics TEM (FEI CM 20 microscope (Netherlands) with a LaB6 cathode, operated at 200 kV, equipped with an Oxford Model 6767 EDS-system (England); FEI Tecnai G^2 S-TWIN microscope with a LaB_6 cathode, a Gatan MS 794 P CCD camera and EDS detector, operated at 200 kV): The tube-containing templates were embedded in Araldit 502© (polymerization at 60°C for 16 h) and examined as

ultrathin sections (70 nm, Reichert-Jung Ultracut E ultramicrotome, DKK diamond knife). SEM (JEOL JSM-7401F, 5–10 kV acceleration voltage): Prior to the measurement, the polymer template was removed with dichloromethane. The freed metal structures were collected on silicon wafer pieces sputter-coated with a thin Au film. XRD (Seifert PTS 3003): Investigations on Cu-NT containing membranes were performed using a Cu anode and an x-ray mirror primary to the sample. At the secondary side, a slit system and a soller 45 slit was used. UV-Vis spectroscopy (ATi Unicam UV/Vis Spectrometer UV4): The measurements were performed on twice ethanol washed template strips in ethanol-filled quartz cuvettes. For the template modification, the standard Sn(II) and Ag(I) baths were used besides a chloride-free Sn(II)-solution (0.042 M $Sn(CH_3SO_3)_2$, 0.071 M CF_3COOH in methanol:water = 1:1) and a sodium chloride solution (0.084 M NaCl, 0.071 M CF_3COOH in methanol:water = 1:1). The shown UV-Vis spectra are substracted from the absorptions of the cuvette, the polycarbonate membrane and the ethanol. They were normalized at 800 nm.

3 Results & discussion

3.1 Ag activation of ion track etched polycarbonate

The protocol for the synthesis of metal-NTs reported by Martin et al. [1, 2] consists of a series of redox reactions. Before electroless metal plating can be applied, Ag-NPs are anchored to the template surface to ensure initial catalytic activity. The Ag-NP deposition is performed by a facile two-step reaction under ambient conditions (room temperature, presence of oxygen). Firstly, the polycarbonate membrane is immersed in a solution containing $SnCl_2$ in which the polar functional groups of the polymer (phenolic hydroxy groups, carbonic acid esters) bind Sn(II)-ions (sensitization). After removal of the supernatant Sn(II) solution, the impregnated template is transferred to a Ag(I)-containing solution. Here, the bound Sn(II) ions cause the precipitation of Ag-NPs on the polymer surface (activation, see (1)). Figure 1 sums up the processing steps and corresponding relevant chemicals required for the growth of metal-NTs inside the ion track etched polymer templates.

$$2Ag(I) + Sn(II) \rightarrow 2Ag + Sn(IV) \quad (1)$$

The catalytically active Ag-NPs act as nuclei for the electroless metal deposition. A high coverage should lead to a low nucleation distance of the plated metal-NPs and improve the formation of dense metal films. According to the standard procedure, the sensitization-activation steps are performed once only [3, 8, 16, 17]. In order to reach a close coverage of the polycarbonate surface with Ag-NPs, the sensitization and activation steps were repeated several times.

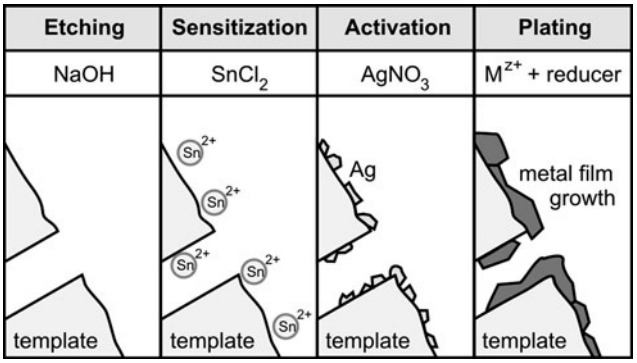

Fig. 1 Reaction route for the electroless synthesis of metal-NTs: Ion track etching with sodium hydroxide solution, template sensitization with Sn(II), Ag-NP activation with Ag(I) and finally electroless metal deposition

The morphology and chemical composition of the deposits on the polymer surface were analyzed as microtome cuts using TEM, SEM and EDS (Fig. 2). EDS (Fig. 2a) confirms that Ag is the main component of the deposited material next to minor fractions of incorporated educts (Sn, Cl). Especially, the most filigree nanostructures are sensitive toward dislocation during to the cutting process, as can be seen in Fig. 2b (the dashed line marks the probable NT cross section; the arrow indicates a displaced piece of the NT wall). Since the microtome cutting cannot be performed accurately perpendicular to the tubes, deviations from the expected cylindrical pore shape are found (white arrows in Fig. 2c). Despite the partial interruption of the Ag film, it can be stated that single activation is able to densely cover the template surface with small Ag-NPs of less than 10 nm size (Fig. 2b). The assumption that the locally found coherent NP films are representative for the whole polycarbonate surface is supported by the formation of complete, homogeneous metal films in consecutive electroless plating (see Sect. 3.2.1). In the case of fivefold activation, more inhomogeneous films of about 30 nm thickness were produced which additionally contained larger particles of 15–30 nm size (Fig. 2c). It is evident that the Ag deposition continued even after the polymer was densely coated with Ag-NPs. In case of a tenfold repeated activation procedure, a rough Ag film was found on the polymer surface, accompanied by Ag-nanowires inside the template (Fig. 2d). The direct reaction of the sensitization and activation solutions can be ruled out due to the washing steps between the transfer of the template membrane. Further, the Ag film growth cannot be solely attributed to the functional groups of the polymer because it continues even after the complete covering of the template surface. We conclude that the Ag-NPs are involved in the growth process. These results allow the synthesis of Ag-NP films of adjustable thickness for future use.

The plasmon resonance of metal-NPs responds strongly to their density, shape, and size as well as to chemical and

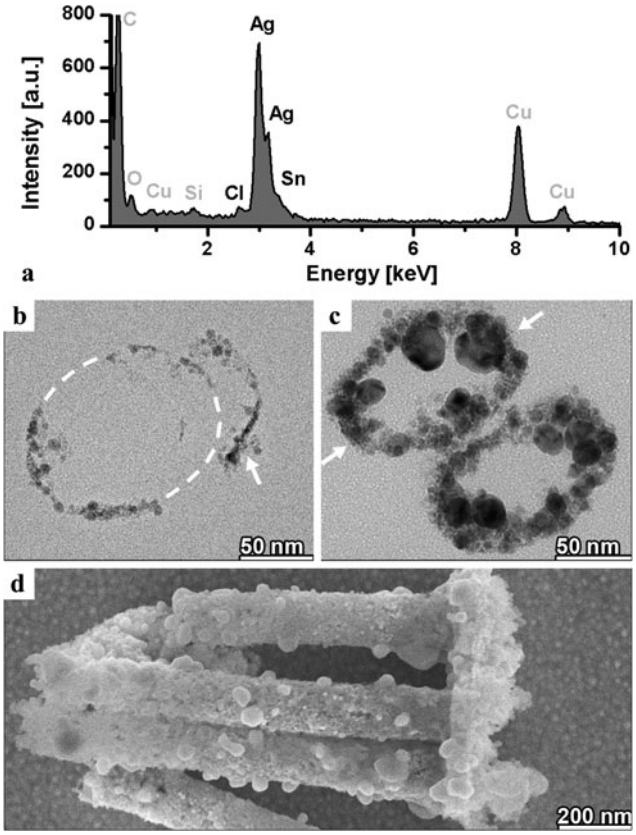

Fig. 2 (**a**) EDS spectrum of the Ag nanostructures obtained by activation. The C and O signals are related to the organic matrix, the Cu signal stems from the TEM grid. (**b**, **c**) TEM-images of Ag-NPs deposited in a polycarbonate nanochannel after single (**b**) and fivefold (**c**) activation (**d**) SEM image of Ag nanowire fragments obtained by tenfold activation

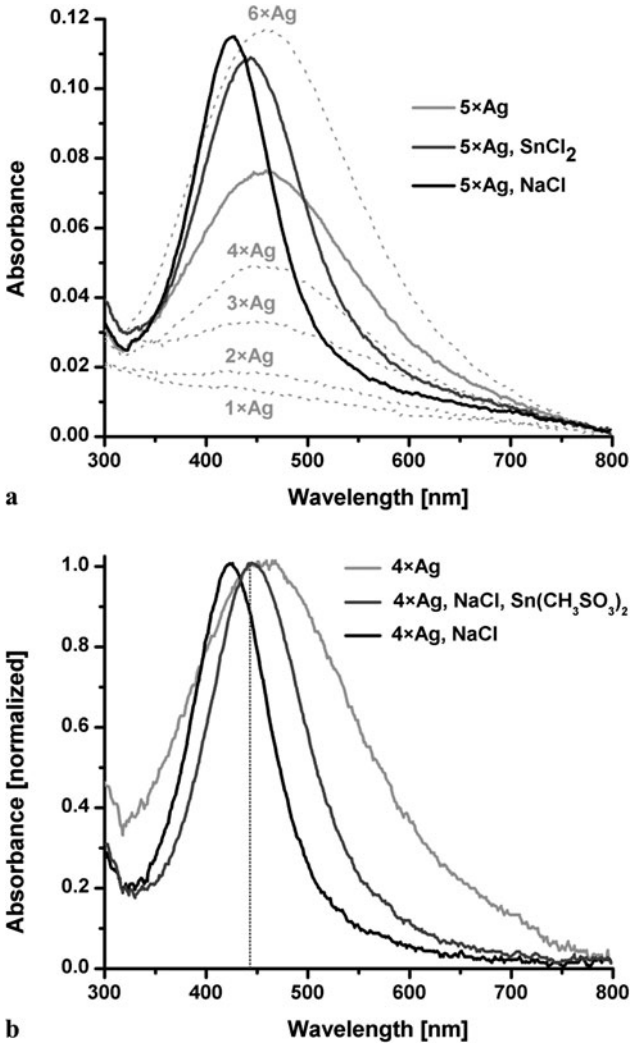

Fig. 3 UV-Vis spectra of activated polycarbonate foils, the figures equal the number of sensitization-activation cycles. (**a**) Spectra of polycarbonate membranes covered with different contents of Ag-NPs. Fivefold activated samples were brought in contact with different electrolytes (solutions of $SnCl_2$ and NaCl). (**b**) Normalized UV-Vis spectra of Ag-covered membranes which have been treated with NaCl solution, followed by a solution of Sn(II)-methanesulfonate. The *dotted line* denotes the peak maximum of the $SnCl_2$-treated sample shown in (**a**)

physical surface changes [18, 19]. To follow the growth process of the Ag-NP thin films, UV-Vis spectra were recorded and evaluated (Fig. 3a). In addition, the obtained Ag nanostructures were treated with different electrolytes in order to relate spectral shifts to the contact to relevant ionic species (Fig. 3a and 3b).

We observed that the brownish color of the template foils deepens with increasing Ag loading. In the UV-Vis spectra this observation is reflected by an intensity increase of the unusually broad and red-shifted Ag plasmon peak with its maximum located around 460 nm (Fig. 3a). A color change to orange-yellow is observed after a Ag-NP covered foil has been transferred back to the $SnCl_2$ solution. The corresponding UV-Vis spectrum ($5\times$Ag, $SnCl_2$) shows a clearly shifted absorption peak (17 nm blue-shift) of increased intensity and reduced width. If the Ag-NP covered foil is immersed in a NaCl solution of the same chloride concentration as the previously used $SnCl_2$ solution, the shift of the absorption peak is more pronounced (35 nm blue-shift).

Due to the high affinity of Ag toward halides, layers of specifically adsorbed halide anions are easily formed on the Ag surface [20]. Plasmon shifts can be ascribed to the formation of adsorbate layers which change the dielectric constant of the particle-surrounding medium or interfere with the electronic structure of the particle itself [18, 19]. The introduction of electronic charge to a particle leads to blue-shifted peaks with increased intensity [19]. Our observations can be explained by taking charge effects into account which resemble the processes occurring during the Fajans titration [21]: In the presence of the $[Ag(NH_3)_2]^+$-containing activation solution, a transfer of positive charge is expected by complex particle interactions. Like in the similar case of $[Ag(CN)_2]^-$-adsorption, the electron density of

Ag-NPs may decrease, reducing their plasma frequency and red-shifting their plasmon band [22].

In the chloride-containing solution, the Ag(I)-ions are substituted and the polarization adopts more negative values. The cathodization of the Ag-NPs leads to a compressed, blue-shifted plasmon peak, as seen in Fig. 3a [19]. Additional effects can be related to the coexistence of counter-cations. Compared to the results of the $SnCl_2$ solution, in the presence of Na(I)-cations a more distinct blue shift is observed corresponding to a higher negative charge (Fig. 3a). This indicates a lower screening effect of the weakly interacting Na(I) cation. In another experiment, the Ag-NPs were consecutively brought into contact with chloride and Sn(II)-ions. For that purpose, an activated foil was immersed in a NaCl solution, thoroughly washed with ethanol and finally transferred to a chloride-free Sn(II) solution. Methanesulfonate was chosen as the Sn(II) counter-anion based on its weak affinity toward silver. The as-obtained UV-Vis spectrum (Fig. 3b) has a peak maximum close to that of the fivefold activated Ag-NP sample which was directly modified with $SnCl_2$. Probably, the consecutive treatment with chloride and Sn(II) leads to an adsorbate structure involving Sn(II), similar to that of Ag-NPs which were brought into contact with $SnCl_2$ solution.

In summary, the Ag film growth occurring on Ag-NPs is explained by the redox reaction of Sn(II)- and Ag(I)-ions which are carried to the solution of the other ion type in form of adsorbates. They are not removed by washing and undergo reactions once in contact with adequate species, leading the continuing precipitation of Ag-NPs according to (1). This successive ionic layer adsorption and reaction (SILAR) process [23] enables the fabrication of Ag-NP films with variable thickness and allows tuning the activity of polymer substrates towards electroless metal deposition.

3.2 Impact of activation on the growth of metal nanotubes

The Ag-NPs precipitated on the polycarbonate surface act as the nuclei for the electroless metal deposition. A high Ag loading has the advantage of a dependable initiation of the metal deposition reaction on the template surface. As critical issues, deposition inhomogeneities and contamination of the resulting structures by the Ag-NP film can be subsumed. Therefore, a balance between an evenly and sufficiently activated surface and the introduction of excess Ag and additional roughness has to be found. Due to the differing catalytic activities of Ag-NPs towards varying plating baths and due to possible side reactions (e.g., cementation of a more noble metal on the Ag-NPs according to the general equation $nAg + M(n+) \rightarrow M + nAg(I)$), a suitable activation has to be optimized in conjunction with a given plating procedure. This will be demonstrated on the basis of two previously reported plating procedures for Au- and Pt-NTs and a new synthesis for Cu-NTs.

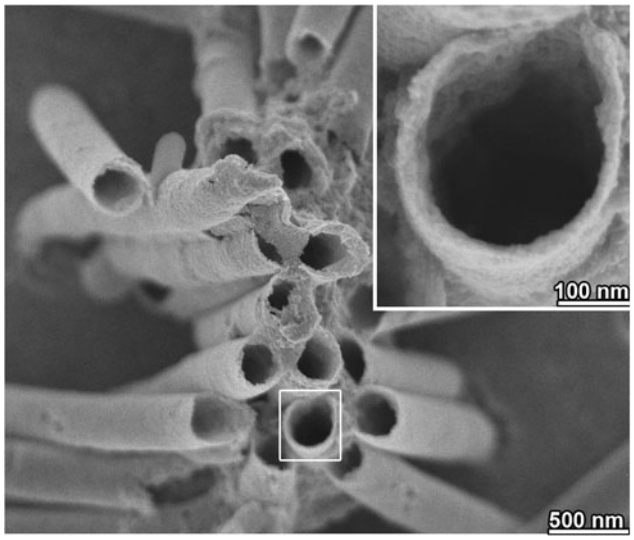

Fig. 4 SEM image of Au-NTs of 300 nm diameter grown in ion track etched polycarbonate. The inset shows a magnified part of the image, highlighting the thin, homogeneous and dense wall structure of the Au-NT

3.2.1 *Formation of gold nanotubes in activated polycarbonate templates*

Polycarbonate-embedded Au-NTs were amongst the first metal-NTs to be synthesized [2]. Nanoscopic Au possesses interesting properties such as chemical resilience, catalytic activity [9], and straightforward surface modifiability with thiols [8]. These benefits lead to the implementation of Au-NTs as separation devices [8] and nanoreactors [9].

For the electroless synthesis of Au-NTs a refined plating bath utilizing Au(I) as the oxidizing agent, sulfite as the ligand, 4-(dimethylamino)pyridine as an additive and formaldehyde as the reducing agent was used [9]. Single activation already allows the plating of a thin and homogeneous Au film to fabricate well defined Au-NTs (Fig. 4). The Au film consists of agglomerated Au-NPs with a small grain size of around 5 nm [9]. Both the reliable initiation of the plating reaction by the Ag-NPs and the small size of the formed Au-NPs are essential for the formation of filigree and closed tube walls. If the Au particles are larger and have higher nucleation distances, thicker films are required until closed NTs are obtained, and very narrow NTs are not accessible [24]. The Ag from the activation is mostly exchanged by the more noble Au during the course of the plating reaction ($Ag + Au(I) \rightarrow Au + Ag(I)$ [3]). As confirmed by EDS in a previously published study [9], even very thin Au films exhibit only traces of Ag.

3.2.2 *Formation of platinum nanotubes in activated polycarbonate templates*

Electroless Pt deposition allows the fabrication of nanostructures acting as efficient catalysts for a wide range of re-

actions (e.g. electroreduction of oxygen, electrooxidation of small organic molecules, etc. [10, 11]). For instance, electrolessly prepared carbon supported Co@Pt core-shell NPs were applied as potent and Pt-saving electrocatalysts [25].

The Pt plating bath consists of $[PtCl_6]^{2-}$ as the oxidizing agent, ethylenediamine as the ligand and hydrazine as the reducing agent. TEM and XRD measurements confirmed that the deposits yielded by this plating baths are composed of nanocrystalline Pt [10]. Compared to the Au plating procedure described above, the reactivity of the Ag-NP covered template surface was much lower. Triple activation was necessary for the formation of robust and free-standing Pt-NTs (Fig. 5a and 5b) after a deposition time of 24 h. In case of single activation, only brittle Pt nanowires were obtained after the extended reaction time of one week (Fig. 5c). The Pt nanostructures are composed of connected, relatively large grains (Fig. 5b). This indicates a relatively high nucleation distance corresponding to less Ag nuclei which are capable of starting the Pt deposition reaction. Both the low activity of the single activated templates and the distance of the Pt grains reveal that a high coverage of Ag-NPs is essential for the formation of a continuous Pt film. In addition, the Ag seeds dissolve in the presence of excess chloride, leaving cavities in the Pt grains [10]. It causes a rough outer tube surface (Fig. 5b) and again points out the distinct influence of the plating solution composition on the reactivity of activated templates. The size of the cavities in the centre of the hemispherical Pt grains indicates that the large Ag-NPs are preferred nuclei for the Pt deposition. This observation is in accordance with the low reactivity of single activated templates which are only covered by a thin layer of small Ag-NPs (Fig. 2b).

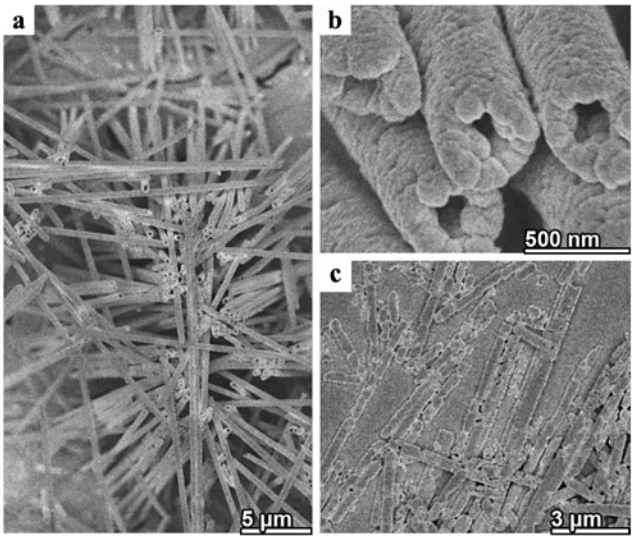

Fig. 5 SEM images of Pt nanostructures grown in differently activated polycarbonate membranes. (**a**) High aspect-ratio Pt-NTs of 500 nm diameter obtained with triple activation alongside (**b**) magnified tube openings. (**c**) Brittle and inhomogeneous Pt nanowires obtained in single activated templates after a reaction time of one week

3.2.3 Formation of copper nanotubes in activated polycarbonate templates

Metallic Cu exhibits characteristics such as unique optical properties or excellent electric conductivity and is a useful reactant for the synthesis of functional multimetallic or oxidic materials. Accordingly, Cu structures as well as their derivatives are applied in diverse nanotechnological fields. For instance, electrolessly prepared Cu thin films and patterns are valuable for microelectronics [26, 27]. Cu films and NPs modified by Ag [28] or Pt [29] were used as highly active and regenerative surface enhanced Raman substrates [28] or fuel cell catalysts for the oxygen reduction reaction [29], respectively. A network consisting of oxidized Cu nanowires could be efficiently implemented as room-temperature operated light, pH, and gas sensors [30].

The dependence of the Ag loading on the Cu-NT growth was tested with a standard electroless Cu plating solution consisting of $CuSO_4$ as the Cu source, tartrate as the ligand and formaldehyde as the reducing agent [13, 15, 27]. The plating solution exhibited high reaction rates and suffered from moderate stability toward homogeneous Cu nucleation. These properties unambiguously hampered the synthesis of narrow Cu-NTs. The reactivity of electroless plating solutions strongly depends on the coordination chemistry of the involved species [11, 17, 31]. For instance, a thermodynamic or kinetic stabilization of the metal complex as the oxidizing component [31] is a straightforward measure to both reduce the rate of heterogeneous deposition and the driving force for homogeneous nucleation. Following this concept, we introduced different ligands to improve the Cu plating results. By adding ethylenediamine as a coligand, the deposition reaction could be clearly controlled. Using an optimized plating solution, homogeneous Cu-NTs of low diameter (down to 300 nm) and high aspect ratio were produced. However, an increased degree of activation was necessary to ensure Cu-NT formation (Fig. 6). In case of triple activation, Cu-NTs completely covering the template length were obtained (Fig. 6a and 6b), whereas single activation only leads to the formation of a Cu film on the outer template surface (Fig. 6c). Thus, the template with single activation exhibits insufficient initial catalytic activity in its nanochannels, while electroless Cu deposition can proceed on the outer surface because of its better accessibility. For a structural and chemical investigation of the Cu nanostructures, additional TEM images, XRD profiles and EDS spectra were recorded (Fig. 7). The plated Cu films are composed of small nanoparticles (Fig. 7b). The crystalline nature of the deposit was verified by XRD, revealing elemental copper to be the dominating phase (Fig. 7c). By EDS (Fig. 7d), traces of sulphur were found in the product (oxygen, carbon and

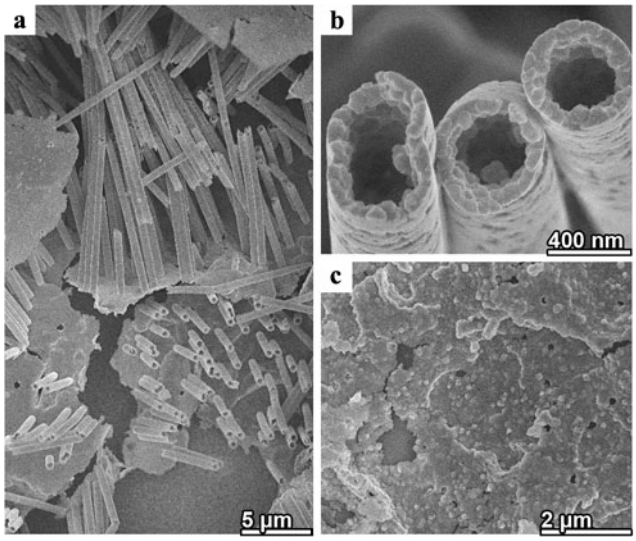

Fig. 6 SEM images of Cu nanostructures grown in polycarbonate membranes. (**a**) Cu-NTs obtained by triple activation. (**b**) Magnified tube openings in the same sample. (**c**) Cu film formation on the outer template surface without significant tube formation was observed in case of single activation

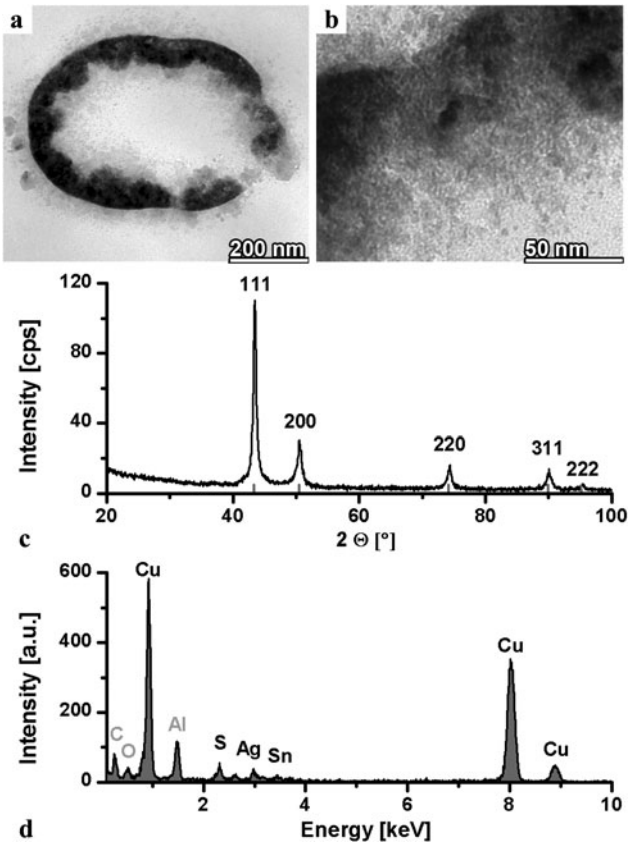

Fig. 7 (**a**) TEM image of Cu-NT microtome cut and magnified part of the tube wall. (**b**) TEM image of a magnified part of the Cu-NT wall. (**c**) XRD pattern of the template-embedded Cu-NTs. All reflexes correspond to metallic Cu. (**d**) EDS spectrum of the Cu nanostructures. The C, O, and Al signals are due to the organic matrix and the TEM grid, the Ag and Sn signals can be related to the activation procedure

aluminum relate to the organic matrix and the TEM grid, respectively). The absence of noticeable oxidic contamination in the Cu-NTs is an important quality criterion since electroless Cu deposits obtained in basic environments or in the presence of certain ligands often contain cuprous oxides [27, 31]. In contrast to the Au plating reaction, the less noble Cu is unable to substitute the Ag nuclei due to the lower Nernst potential (Cu / Cu^{2+} ($E^0 = 0.3419$ V)) compared to Ag / Ag^+ ($E^0 = 0.7996$ V) [32]. Thus, the Sn-containing Ag film stemming from the activation process remains in the Cu structures (Fig. 7d).

4 Conclusions

In our work, we have shown that Ag-NP thin films of varying thickness can be synthesized on polycarbonate substrates by a simple wet-chemical multistep process. From the morphological and spectroscopic results, we highlighted that the reaction relies on species bound to the template and the Ag particle surface, leading to an indirect contact of the used oxidizing and reducing agents (Sn(II) and Ag(I)). Due to the active role of elemental Ag in the transport of reactive species, the described procedure can be applied to arbitrary Ag-terminated surfaces. It is transferrable to other substrates supporting initial Ag-NP formation such as polyethyleneterephthalate or polyimide. Also, the activation protocol can be applied to other template shapes. Based on the high flexibility concerning the substrate material, shape and activation state, the presented method is beneficial for the general synthesis of metal films and nanomaterials by electroless plating.

With regard to the nanostructure formation in ion track etched polycarbonate, we observed a strong dependence on the template activation. An individual optimization of the activation procedure proved to be critical for the successful fabrication of metal-NTs. While Au-NTs already formed in a single activated template, triple activation was necessary for the production of Pt- and Cu-NTs. The electroless Cu plating can be significantly enhanced by the addition of ethylenediamine as a coligand, leading to a reduced reaction rate and increased bath stability.

Metal-NTs are a promising new class of unsupported catalysts [10, 33, 34], and easily accessible Cu-NTs are desired educts for novel catalyst systems. Since mixed Cu-Pt nanostructures show significantly improved activity in the oxygen reduction reaction [29, 35–37], we are now exploring the utilization of Cu-NTs as templates for bimetallic fuel cell catalysts.

Acknowledgements We thank Prof. Reinhard Neumann and Dr. Christina Trautmann (GSI Helmholtz Centre for Heavy Ion Research)

for support with the template preparation and for the possibility to use the SEM and UV-Vis instruments of the materials research group. We also thank the Zentraleinrichtung Elektronenmikroskopie at the Technische Universität Berlin and Ulrike Kunz for TEM and Joachim Brötz for XRD measurements. The supply of gold solution by Schütz Dental GmbH is gratefully acknowledged.

References

1. C.R. Martin, Science **266**, 1994 (1961)
2. C.J. Brumlik, V.P. Menon, C.R. Martin, J. Mater. Res. **9**, 1174 (1994)
3. V.P. Menon, C.R. Martin, Anal. Chem. **67**, 1995 (1920)
4. E. Ferain, R. Legras, Nucl. Instrum. Methods Phys. Res., Sect. B, Beam Interact. Mater. Atoms **174**, 116 (2001)
5. T.W. Cornelius, P.Y. Apel, B. Schiedt, C. Trautmann, M.E. Toimil-Molares, S. Karim, R. Neumann, Nucl. Instrum. Methods Phys. Res., Sect. B, Beam Interact. Mater. Atoms **265**, 553 (2007)
6. C.R. Martin, Z.S. Siwy, Science **317**, 331 (2007)
7. A. Dangwal, C.S. Pandey, G. Müller, S. Karim, T.W. Cornelius, C. Trautmann, Appl. Phys. Lett. **92**, 063115 (2008)
8. K.B. Jirage, J.C. Hulteen, C.R. Martin, Anal. Chem. **71**, 4913 (1999)
9. F. Muench, U. Kunz, C. Neetzel, S. Lauterbach, H.J. Kleebe, W. Ensinger, Langmuir **27**, 430 (2011)
10. F. Muench, S. Kaserer, U. Kunz, I. Svoboda, J. Brötz, S. Lauterbach, H.J. Kleebe, C. Roth, W. Ensinger, J. Mater. Chem. **21**, 6286 (2011)
11. C.R.K. Rao, D.C. Trivedi, Coord. Chem. Rev. **249**, 613 (2005)
12. H.O. Ali, I.R.A. Christie, Gold Bull. **17**, 118 (1984)
13. B. Bercu, I. Enculesco, R. Spohr, Nucl. Instrum. Methods Phys. Res., Sect. B, Beam Interact. Mater. Atoms **225**, 497 (2004)
14. W. Wang, N. Li, X. Li, W. Geng, S. Qiu, Mater. Res. Bull. **41**, 1417 (2006)
15. N. Li, X. Li, X. Yin, W. Wang, S. Qiu, Solid State Commun. **132**, 841 (2004)
16. S. Demoustier-Champagne, M. Delvaux, Mater. Sci. Eng., C, Biomim. Mater., Sens. Syst. **15**, 269 (2001)
17. S. Yu, U. Welp, L.Z. Hua, A. Rydh, W.K. Kwok, H.H. Wang, Chem. Mater. **17**, 3445 (2005)
18. C. Bréchignac, P. Houdy, M. Lahmani, *Nanomaterials and Nanochemistry* (Springer, Berlin, 2007), pp. 197–227
19. P. Mulvaney, Langmuir **12**, 788 (1996)
20. O.M. Magnussen, Chem. Rev. **102**, 679 (2002)
21. I.M. Kolthoff, E.B. Sandell, E.J. Meehan, S. Bruckenstein, *Quantitive Chemical Analysis*, 4th edn. (Collier-Macmillan, London, 1971), p. 721
22. P. Mulvaney, T. Linnert, A. Henglein, J. Phys. Chem. **95**, 7843 (1991)
23. S. Lindroos, T. Ruuskanen, M. Ritala, M. Leskelä, Thin Solid Films **460**, 36 (2004)
24. M. De Leo, F.C. Pereira, L.M. Moretto, P. Scopece, S. Polizzi, P. Ugo, Chem. Mater. **19**, 5955 (2007)
25. K.D. Beard, D. Borrelli, A.M. Cramer, D. Blom, J.W. Van Zee, J.R. Monnier, ACS Nano **3**, 2841 (2009)
26. S.Y. Chang, C.W. Lin, H.H. Hsu, J.H. Fang, S.J. Lin, J. Electrochem. Soc. **151**, C81 (2004)
27. T. Asher, A. Inberg, E. Glickman, N. Fishelson, Y. Shacham-Diamand, Electrochim. Acta **54**, 6053 (2009)
28. Y. Lai, W. Pan, D. Zhang, J. Zhan, Nanoscale **3**, 2134 (2011)
29. A. Sarkar, A. Manthiram, J. Phys. Chem. C **114**, 4725 (2010)
30. M. Kevin, W.L. Ong, G.H. Lee, G.W. Ho, Nanotechnology **22**, 235701 (2011)
31. R. Pauliukaitė, G. Stalnionis, Z. Jusys, A. Vaškelis, J. Appl. Electrochem. **36**, 1261 (2006)
32. D.R. Lide, *Handbook of Chemistry and Physics*, 84th edn. (CRC Press, Boca Raton, 2003–2004), pp. 23–33
33. Z. Chen, M. Waje, W. Li, Y. Yan, Angew. Chem., Int. Ed. Engl. **46**, 4060 (2007)
34. E. Antolini, J. Perez, J. Mater. Sci. **46**, 4435 (2011)
35. M. Oezaslan, P. Strasser, J. Power Sources **196**, 5240 (2011)
36. M. Oezaslan, F. Hasché, P. Strasser, Chem. Mater. **23**, 2159 (2011)
37. P. Strasser, S. Koh, T. Anniyev, J. Greeley, K. More, C. Yu, Z. Liu, S. Kaya, D. Nordlund, H. Ogasawara, M.F. Toney, A. Nilsson, Nat. Chem. **2**, 454 (2010)